Journal of Advanced Research 27 (2021) 177–190

Contents lists available at ScienceDirect

Journal of Advanced Research

journal homepage: www.elsevier.com/locate/jare

Research Article

Targeting hydrogen sulphide signaling in breast cancer

Rana Ahmed Youness [a], Ahmed Zakaria Gad [b,c,d,e], Khaled Sanber [c,d,f], Yong Jin Ahn [g,h], Gi-Ja Lee [g,h], Emad Khallaf [i], Hafez Mohamed Hafez [i], Amira Abdel Motaal [j,k], Nabil Ahmed [b,c,d,e,l], Mohamed Zakaria Gad [m,*]

[a] Department of Pharmaceutical Biology, Faculty of Pharmacy and Biotechnology, German University in Cairo, Egypt
[b] Interdepartmental Program in Translational Biology and Molecular Medicine, Baylor College of Medicine, Houston, TX 77030, USA
[c] Center for Cell and Gene Therapy, Texas Children's Hospital, Houston Methodist Hospital, Baylor College of Medicine, Houston, TX 77030, USA
[d] Texas Children's Cancer and Hematology Centers, Texas Children's Hospital, Baylor College of Medicine, Houston, TX 77030, USA
[e] Department of Pediatrics, Baylor College of Medicine, Houston, TX 77030, USA
[f] Department of Medicine, Baylor College of Medicine, Houston, TX 77030, USA
[g] Department of Medical Engineering, Graduate School, Kyung Hee University, Seoul 130-701, Republic of Korea
[h] Department of Biomedical Engineering, College of Medicine, Kyung Hee University, Seoul 130-701, Republic of Korea
[i] Department of General Surgery, Faculty of Medicine, Cairo University, 12613 Cairo, Egypt
[j] Department of Pharmacognosy, College of Pharmacy, King Khalid University, Abha, Saudi Arabia
[k] Department of Pharmacognosy, Faculty of Pharmacy, Cairo University, Egypt
[l] Department of Pathology and Immunology, Baylor College of Medicine, Houston, TX 77030, USA
[m] Department of Biochemistry, Faculty of Pharmacy and Biotechnology, German University in Cairo, Egypt

GRAPHICAL ABSTRACT

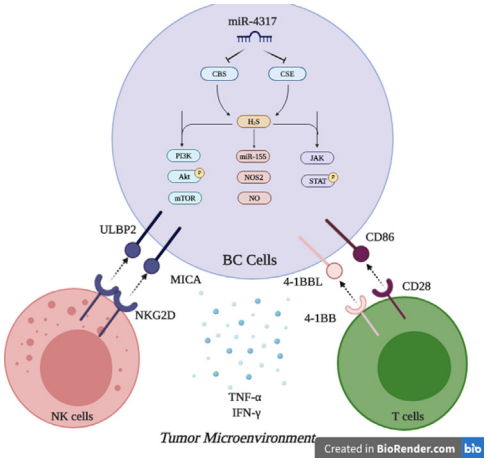

Abbreviations: BC, Breast Cancer; CAR, Chimeric antigen receptor; ^{51}Cr-release, Chromium release assay; CD80, Cluster of differentiation 80; CD86, Cluster of differentiation 86; CBS, Cystathionine β-synthase; CSE, Cystathionine γ-lyase; CTL, Cytotoxic T lymphocyte; NOS3, Endothelial nitric oxide synthase-3; HCC, Hepatocellular carcinoma; HLA-DR, Human Leukocytic antigen DR; H_2S, Hydrogen sulphide; NOS2, Inducible nitric oxide synthase-2; IFN-γ, Interferon gamma; KD, Knock down; LDH, Lactate dehydrogenase Assay; MICA/B, MHC class I polypeptide-related sequence A/B; miRNA, MicroRNA; NKG2D, Natural Killer Group 2D ; NK, Natural killer; NO, Nitric oxide; ncRNAs, Non-coding RNAs; PD-L1, Programmed death-ligand 1; Scr-miRNAs, Scrambled microRNAs; Scr-siRNAs, Scrambled siRNAs; siRNAs, Small interfering RNAs; TNBC, Triple negative breast cancer; TNF-α, Tumor necrosis factor-α; ULBP2/5/6, UL16 binding protein 2/5/6; 41BBL, 41BB Ligand.

Peer review under responsibility of Cairo University.

* Corresponding author.
E-mail addresses: rana.ahmed-youness@guc.edu.eg (R.A. Youness), mohamed.gad@guc.edu.eg (M.Z. Gad).

https://doi.org/10.1016/j.jare.2020.07.006
2090-1232/

ARTICLE INFO

Article history:
Received 20 April 2020
Revised 6 July 2020
Accepted 12 July 2020
Available online 16 July 2020

Keywords:
Breast cancer
Hydrogen sulphide
miR-155/NOS2/NO signaling pathway
PI3K/AKT signaling pathway
Nitric oxide
miR-4317
Natural killer cells
CAR T cells

ABSTRACT

Introduction: Hydrogen sulphide (H_2S) has been established as a key member of the gasotransmitters family that recently showed a pivotal role in various pathological conditions including cancer.
Objectives: This study investigated the role of H_2S in breast cancer (BC) pathogenesis, on BC immune recognition capacity and the consequence of targeting H_2S using non-coding RNAs.
Methods: Eighty BC patients have been recruited for the study. BC cell lines were cultured and transfected using validated oligonucleotide delivery system. Gene and protein expression analysis was performed using qRT-PCR, western blot and flow-cytometry. *In-vitro* analysis for BC hallmarks was performed using MTT, BrdU, Modified Boyden chamber, migration and colony forming assays. H_2S and nitric oxide (NO) levels were measured spectrophotometrically. Primary natural killer cells (NK cells) and T cell isolation and chimeric antigen receptor transduction (CAR T cells) were performed using appropriate kits. NK and T cells cytotoxicity was measured. Finally, computational target prediction analysis and binding confirmation analyses were performed using different software and dual luciferase assay kit, respectively.
Results: The H_2S synthesizing enzymes, cystathionine β-synthase (CBS) and cystathionine γ-lyase (CSE), exhibited elevated levels in the clinical samples that correlated with tumor proliferation index. Knockdown of CBS and CSE in the HER2+ BC and triple negative BC (TNBC) cells resulted in significant attenuation of BC malignancy. In addition to increased susceptibility of HER2+ BC and TNBC to the cytotoxic activity of HER2 targeting CAR T cells and NK cells, respectively. Transcriptomic and phosphoprotein analysis revealed that H_2S signaling is mediated through Akt in MCF7, STAT3 in MDA-MB-231 and miR-155/ NOS2/NO signaling in both cell lines. Lastly, miR-4317 was found to function as an upstream regulator of CBS and CSE synergistically abrogates the malignancy of BC cells.
Conclusion: These findings demonstrate the potential role of H_2S signaling in BC pathogenesis and the potential of its targeting for disease mitigation.

Introduction

Breast cancer (BC) is the most common malignancy in females and the leading cause of cancer-related mortailty [1,2]. BC incidence and mortality rates widely vary in countries with different socio-economic levels, with estimated incidence rates of 54.4% and 31.3% in developed and developing countries, respectively [2]. BC presents as diverse BC subtypes, which differ in prognosis and treatment options, reflecting disease heterogeneity. Hormone receptor (HR) positive tumors show high response rates to hormonal therapies. Human epidermal growth factor receptor 2 (HER2) positive tumors are amenable for treatment using HER2 targeting antibodies and HER2 specific tyrosine kinase inhibitors [3]. For triple negative breast cancer (TNBC), targeted treatment options are limited and outcomes have been substantially worse [4–6]. *Collectively*, this underscores BC, and particularly TNBC, as a significant worldwide problem in dire need for more efficacious and innovative therapies [7,8].

Hydrogen sulfide (H_2S) is a recently identified member of a well-characterized family of gaseous biological mediators, known as gasotransmitters [9]. Since its discovery, endogenous H_2S has been proven to play pivotal roles in various physiological and pathological conditions [10]. In cancer, we and others have recently reported that H_2S acts as a key player in modulating several canonical and non-canonical oncogenic signaling pathways such as PI3K/AKT/mTOR [11], JAK/STAT [12,13], Ras/Raf/MEK/ERK [11], and nitric oxide (NO) [14] signaling cascades. Our group also highlighted the regulatory effects of H_2S on the non-coding RNA (ncRNA) machinery in BC cells [14,15].

The H_2S synthesizing enzymes, cystathionine β-synthase (CBS) and cystathionine γ-lyase (CSE), have been reported to have an organ- and tissue- specific expression pattern. High expression profiles of CBS and CSE have been linked to the aggressiveness of several solid tumors, but are generally expressed at lower levels in hematological malignancies [16,17]. For instance, upregulation of CBS was reported in androgen-dependent prostate, colon and ovarian cancer cells [18,19]. The latter two showed increased H_2S production when compared to non-malignant epithelial cells. In contrary, the expression level of CBS has been described to be significantly low in hepatocellular carcinoma (HCC) [18,20]. Although CBS expression tends to be higher in most of the solid tumors, variability between patients with different histopathologic malignancies suggests the need for further molecular characterization of tumors. CSE was also found to enhance cellular proliferation and migration of colon cancer cell lines [21–23]. Similarly, in HCC, prostate cancer and glioma cell lines, endogenous H_2S produced by CSE has been involved in the survival and proliferation of these malignant cell lines [24–26]. *Collectively*, CBS and CSE expression patterns and functional correlations have been reported in different solid tumors, but their role in BC is yet to be clarified.

In the present study, we aim to evaluate the expression patterns of H_2S synthesizing enzymes in a cohort of BC patients, to unravel the mechanisms by which H_2S modulates the oncogenic and the immunogenic properties of BC cells, and lastly to explore the therapeutic potential of targeting H_2S synthesizing enzymes using ncRNAs.

Materials and methods

Study patients

BC tissues and normal breast tissues were surgically resected from 80 female patients with BC. Tumor and normal tissues were morphologically proven by a pathologist. Classification of the BC patients according to clinical data is provided in Table 1. Detailed immuno-histochemical and pathological profiles of patients are provided in (Supplementary Table S1). Fifty healthy donors were also recruited in this study. All performed experiments are compliant with the guidelines of the Institutional Review Board of Kasr El Aini Medical School, Cairo University and German University in Cairo and with the ethical standards of the declaration of Helsinki

Table 1
Clinical data summary of the recruited female BC patients.

BC patients		Percentage (Count)
Age (Years)	≥40	**73.75%** (59/80)
	<40	**26.25%** (21/80)
Grade	I	**3.75%** (3/80)
	II	**77.5%** (62/80)
	III	**18.75%** (15/80)
Histological type	Ductal	**96.25%** (77/80)
	Lobular	**1.25%** (1/80)
	Both	**2.5%** (2/80)
Molecular Subtype	Luminal A	**22.5%** (18/80)
	Luminal B	**43.75%** (35/80)
	HER-2 enriched	**2.5%** (2/80)
	TNBC	**31.25%** (25/80)
ER/PR status	Positive	**66.25%** (53/80)
	Negative	**33.75%** (27/80)
HER2 status	Positive	**26.25%** (21/80)
	Negative	**73.75%** (59/80)
Lymphatic involvement	Yes	**66.25%** (53/80)
	No	**33.75%** (27/80)
Proliferation Index (Ki-67)	High (≥14%)	**70%** (56/80)
	Low (<14%)	**30%** (24/80)

ER: estrogen receptor; PR: progesterone receptor; HER2: human epidermal growth factor receptor 2.

(Ethical Approval Number: N-70-2016). All participants were included after giving written informed consents.

Cell culture and treatment

MDA-MB-231 and MCF-7 BC cell lines were obtained from ATCC and Vacsera, Egypt. BC cells were cultured in DMEM (Lonza, Switzerland) media as previously described [14,27–29].

Oligonucleotides transfection

Breast cancer cells were transfected using different oligonucleotides (such as: CBS siRNAs, CSE siRNAs, miR-4317 mimics, scrambled siRNAs (Scr-siRNAs), scrambled miRNAs (Scr-miRNAs)) (Qiagen, Germany). All transfection experiments were executed in triplicates employing HiPerfect Transfection Reagent (Qiagen, Germany). All Experiments were repeated 3 times or more [14,28,30,31].

Cellular viability and proliferation experiments

3-(4, 5-dimethylthiazol-2-yl)-2,5-diphenyltetrazolium bromide (MTT) reagent was used for the cellular viability experiments. BC cells (10,000 cells) were seeded in 200 μL media in a 96-well plate. Post-transfection, 48 h later media in each well was replaced by 20 μL working solution. After 6 h, the absorbance of the formazan crystals, solubilized in 200 μL buffer, was measured [14,27,28,30]. Bromo-deoxyuridine (BrdU) incorporation assay was used for the proliferation experiments. BC cells were seeded into black 96-well plates at a cell density of 5×10^4 cells/well. In accordance with the Cell Proliferation ELISA kit (Roche Applied Science, Penzberg, Germany), BC cells were incubated with BrdU for 4 h, then fixed using Fix-Denate for 30 min and incubated with Anti-BrdU POD for 90 min [14,27,28,30]. All experiments were performed in triplicates and repeated 3 times or more.

Cellular migration and invasion

Wound-healing assay was done to assess BC cellular migration. Transfected cells were left to grow to a confluency of 90–95% in 24-well plates. Post-transfection, 3 scratches were made in each well using a 10- μL pipette tip. Cells were washed using PBS and replenished with new low-serum media (1% FBS). Twenty four hours later, the surface areas of the scratches were measured and wound closure was quantified with Zen2012 software [14,27,28,30]. The Modified Boyden chamber assay (BD Bioscience, Bedford, USA) was done to assess the *in-vitro* invasion capacity. In 24-well plates, BC cells were transfected with different oligonucleotides. After transfection, 6×10^4 cells, re-suspended in 200 μL low-serum media (1% FBS), were seeded in the upper well, while the lower well contained high-serum media (20% FBS). Cells were washed from the upper surface using a cotton swab 8 h later. The transwell migrant cells were fixed and stained using 1% crystal violet (Sigma Chemical Co., California, USA) and then counted under an inverted light microscope. All experiments were performed in triplicate and repeated 3 times or more [6,14,27].

Colony-forming assay

For the colony forming assay, 48 h post-transfection, cells were harvested and seeded in 6-well plate at a count of 900 cells/well. Cells were incubated in full DMEM under normal conditions (37 °C and 5% CO_2) for 2–3 weeks. Colonies were fixed using 6% glutaraldehyde, stained by 0.05% crystal violet and then manually counted [14,27,32].

Total RNA and miRNAs extraction

Biazol reagent was used for total RNA and miRNAs extraction from primary tissues and cell lines. RNA integrity was examined by 18 s rRNA bands detection on 1% agarose gel electrophoresis. RNA samples were examined for possible contamination with other molecules such as proteins, cellular fragments, or organic compounds using spectrophotometric analysis. The harvested RNA samples were spectrophotometrically assessed at two different wavelengths (260 and 280 nm) to assess its purity. The 260/280 ratio is used to assess the amount of protein contamination which could be present in trace amount during the process of RNA isolation. A ratio of ~ 2.0 is generally accepted as "pure" for RNA. If the ratio is appreciably lower, it may indicate the presence of protein, phenol or other contaminants that absorb strongly at or near 280 nm [14,27,28,30,33].

Quantitative real-time PCR analysis

Reverse transcription of CBS, CSE, NOS2, NOS3, MICA, ULBP2, TNF-α, IFN-γ, β-actin and 18srRNA mRNAs into cDNA was done using the High-Capacity cDNA Reverse Transcription Kit (ABI, California, USA) according to the manufacturer's instruction. The extracted miRNAs were reverse transcribed into single-stranded complementary DNA (cDNA) using TaqMan MicroRNA Reverse Transcription Kit (ABI, California, USA) and specific primers for hsa-miR-155, hsa-miR-146, hsa-miR-4317 and RNU6B. Relative expression of CBS, CSE, NOS2, NOS3, MICA, ULBP2, TNF-α, IFN-γ, β-actin and 18 s rRNA (for normalization), miR-155, miR-146a, miR-4317 and RNU6B (for normalization) was quantified using TaqMan Real-Time q-PCR on StepOne™ Systems (ABI, California, USA). Relative expression was calculated using the $2^{-\Delta\Delta Ct}$ method. All PCR reactions were done in triplicates and repeated 3 times or more [14,27,28,30,34].

Western blot analysis

Post oligonucleotides transfection, BC cells were lysed using RIPA lysis buffer (Pierce Biotechnology, Massachusetts, United States) containing Protease Inhibitor Cocktail Set III and Phosphatase Inhibitor Cocktail Set II (EMD Biosciences, California, USA). BCA protein assay kit (Pierce Biotechnology, Massachusetts,

USA) was adopted to determine the concentration of proteins. Protein lysates (25–35 μg) were diluted with 4x laemmli buffers and incubated for 10 min at 95 °C. Proteins were then separated on 12% SDS-PAGE gels in mini electrophoresis system (Bio-Rad Laboratories, California, USA). Amersham™ ECL™ Rainbow™ Marker - Full range (GE Healthcare, California, USA) was applied as a protein size detection marker. Separated proteins were then transferred to iBlot™ 2 Transfer Stack nitrocellulose membranes (Life Technologies, California, USA) using an iBlot™ 2 dry transfer system (Life Technologies, California, USA). Membranes were blocked for 1 h using 5% fat-free dry milk in TBS (Bio-Rad Laboratories, California, USA) supplied by 0.1% tween 20 (Sigma-Aldrich, California, USA) then incubated over-night with CBS (ab140600, Abcam, California, USA), CSE (ab54573, Abcam, California, USA), Akt (pan) (Cell Signaling Technology), Phospho-Akt (s473) (Cell Signaling Technology), Phospho-STAT3 (y705) (BD Biosciences/ Cell Signaling Technology) and GAPDH (Cell Signaling Technology, California, USA) antibodies. Fluorophore labeled IRDye® (LI-COR Biosciences, California, USA) secondary antibodies were used for protein detection. Fluorescence visualization was done using an Odyssey CLx membrane imaging system (LI-COR Biosciences, California, USA). All western blot experiments were done in triplicates and repeated at least 3 times [6].

Quantification of H_2S production

A microplate colorimetric H_2S detection assay designed for H_2S measurement was used as previously described [35,36]. Briefly, poly vinyl pyrrolidone (PVP, 5% w/v) solution was added to Nafion® perfluorinated resin solution in a ratio of 9:1 (v/v). Thirty μL of 0.1 M silver nitrate (AgNO3) was then combined with the Nafion/PVP mixture. The Ag/Nafion/PVP solution was vortexed, and then 20 μL of solution was dropped per carefully on the lower side of the cover. The cover was dried for at least 3 h to form a membranous coating. To obtain calibration curve, 300 μL of the freshly prepared Na_2S solution, at concentrations ranging from 6.25 to 50 μM, was added to a 96-well plate. The plate was covered with the fabricated Ag/Nafion/PVP coated cover. H_2S was allowed to form Na_2S for 4 h at 37 °C in a 5% CO_2 incubator. The absorbance at 310 nm was measured using a Synergy HTX multi-mode reader (BioTek, Winooski, VT, United States). Next, we analyzed the absorbance of the Ag/Nafion/PVP membrane for H_2S produced from BC cells. Finally, H_2S concentration was calculated against the calibration curve (sensitivity: 0.0049 Abs/μM H_2S). AgNO3, PVP (K90), Nafion® perfluorinated resin solution, Na_2S, GSH, DTT, H-Cys and Cys were purchased from Sigma Aldrich (California, USA).

Quantification of NO production

NO production was measured using Griess reagent assay (Promega, USA) [14]. Briefly, 50 μL of cell culture supernatant mixed with 50 μL of the sulfanilamide solution were incubated for 10 min. Fifty μL of N-1-napthylethylenediamine dihydrochloride (NED) solution were then added and absorbance was measured at 540 nm using Wallac 1420 Victor 2 Multilabel Counter (Perkin Elmer, USA). Experiments were performed in triplicates and repeated 3 times or more [14].

Detection of cell surface markers using flow cytometry

After oligonucleotides transfection according to the manufacturing protocol, tumor cells were trypsinized then washed with cold PBS. Cells were immunostained for 45 min – 1 h with fluorophore-conjugated primary antibodies. Antibodies used included: anti-HER2_FITC, anti-HLA-DR_FITC, anti-CD80_PE, anti-CD86_APC (BD Biosciences, San Jose, California, USA), and PD-L1_PE-Cy5 (BioLegend, California, United States). CAR expression was detected by immunostaining with a recombinant human ErbB2/Her2 Fc chimeric protein (R&D Systems) at 4 °C for 1 h followed by a PE-conjugated goat anti-human IgG (Fc gamma-specific) (eBioscience). Cells were analyzed on Accuri C6 or BD Canto II flok6w cytometers (BD bioscience, California, USA). Data analysis was done using FlowJo™ 10 (BD bioscience, California, USA) [31].

NK cell isolation

Peripheral blood mononuclear cells (PBMCs) were separated from peripheral blood of healthy donors within 4 h of collection using Ficoll–Hypaque centrifugation (Axis-Shield PoC AS, Norway). NK cells were then enriched by negative selection using a MACS NK cell isolation kit (Miltenyi Biotec, Cologne, Germany). Enriched NK cell populations were 97.4% CD56/CD3 and 1.2% CD3 positive, assessed by flow cytometry [14,28,37].

NK cell-mediated cytolytic assay

MDA-MB-231 cells transfected with different oligonucleotides were seeded in a U-shaped 96-well plate at a cell density of 15,000 cells/well. After 2 h, primary NK cells were added to the target MDA-MB-231 cells at a 5:1 effector to target ratio (E:T) and incubated for 6–8 h. Later, the lactate dehydrogenase (LDH) activity assay kit (MAK066-1 K1-Sigma-Aldrich, St. Louis, MO, USA) was used to measure the *in-vitro* cytotoxicity following the manufacturer's instructions. The percentage of lysis was calculated according to the following equation: % cytotoxicity = (target maximum release – experimental release)/ (target maximum release) × 100. The experiment was done in triplicate and repeated at least 3 times [14,28,37].

T cell isolation and chimeric antigen receptor (CAR) transduction

Chimeric antigen receptor (CAR) encoding γ-retroviruses were produced by co-transfecting 293 T cells with an FRP5.CD28.ζ containing SFG retroviral vector plasmid, a Peq-Pam plasmid, encoding Moloney GagPol, and RD114 envelope containing plasmid using Gene Juice transfection reagent (EMD Biosciences). Supernatants having the pseudo-retroviruses were harvested 72 h later. Briefly, PBMCs were separated from fresh blood of healthy donors, consented by a protocol approved by the IRB of Baylor College of Medicine, using Lymphoprep density gradient media (STEM CELL technologies). PBMCs were activated with CD3 (OKT3 –OrthoBiotech) / CD28 antibodies (BD Biosciences) to stimulate T cell proliferation. Twenty-four hours later, recombinant human interleukin 7 and 15 (IL-7/IL-15) were added. On day 3, cells were harvested for retroviral transduction. CAR encoding γ-retroviruses were centrifuged for 1 h at 3000 g on non-tissue culture–treated 24-well plate coated with recombinant fibronectin (RetroNectin - Takara Bio, USA). Subsequently, 1×10^5 T cells per well were transduced with retroviruses in the presence of IL-7/IL-15, by centrifugation for 5 min at 1000 g. After 48 h, cells were removed.

T cell cytotoxicity assay

Radioactive chromium (^{51}Cr)-release assays were performed. Briefly, MCF-7 cells transfected with different oligonucleotides for 72 h were incubated with ^{51}Cr for 1 h. In v-shaped 96 well plates T cells and BC cells were co-cultured at different concentrations. After 6 h, the supernatant was collected and analyzed for ^{51}Cr. The average cytolysis of triplicate wells = (test release-spontaneous release) / (max release-spontaneous release) × 100.

Bioinformatic analysis

The computational software: miRDB (www.mirdb.org/miRDB), miRanda (www.microrna.org), DIANA Lab (www.diana.cslab.ece.ntua.gr), and Target Scan (www.targetscan.org) were adopted to predict novel miRNAs that could dually target CBS and CSE simultaneously with good binding scores as previously described [28,31,34,37,38]. This software use special algorithms for prediction and the results are based on multiple criteria including miRNA-mRNA complementarity strength, binding score, hybridization energy, and number of predicted binding sites within the transcripts' 3′-UTR and the candidate miRNA. It is important to note that according to miRanda software, the more negative the hybridization energy is, the more favorable the binding between the miRNA and its target transcript. Moreover, complementarity percentage was evaluated manually by calculating how many nucleotides out of the 22 nucleotide-length miRNA were occupied by base pairing with its complementary target sequence on the 3′-UTR of the target genes mRNA.

Reporter constructs and luciferase assay

To confirm the binding of miR-4317 to CBS and CSE 3′-UTR, a dual firefly luciferase reporter construct was utilized (pmirGLO) (Promega, Madison, WI). pmirGLO Dual Luciferase microRNA target expression vector was co-digested using SacI and XbaI restriction enzymes (Thermoscientific, Boston, MA, USA). For wild-type constructs (WT), the miR-4317 binding region in 3′-UTRs of CBS and CSE were inserted in the pmirGLO vector separately. Moreover, mutant constructs (MUT) were designed (Supplementary Table S2). The sequences in bold refer to the binding region nucleotides that were deleted in the mutant constructs. MDA-MB-231 cells were transfected with the constructs or empty pmirGLO vector using SuperFect Tranfection Reagent (Qiagen, Germany) then co-transfected 24 h later with miR-4317 mimics or Scr-miR using HiPerFect Tranfection Reagent (Qiagen, Germany). After 48 h, relative luciferase activity was measured using SteadyGlo luciferase reporter assay kit (Promega, Germany) [14,37].

Statistical analysis

Data is presented as mean ± standard error of the mean (SEM) for at least 3 different experiments, unless otherwise indicated in figure legends. Non-parametric unpaired student-*t*-test was executed to compare between every two independent groups (e.g. screening results). One-way analysis of variance with post hoc analysis was adopted for multiple comparisons (e.g. tranfection experiments). Correlation analysis was performed by Spearman analysis. P-value of < 0.05 was considered statistically significant, and the threshold of significance is denoted by $^{*}= p < 0.05$, $^{**}p < 0.01$, $^{***}= p < 0.001$, $^{****}=p < 0.0001$. Data was analyzed using GraphPad Prism 8.2.1 software.

Results

Breast cancer patients express high levels of CBS, CSE and H_2S

First, we assessed the levels of CBS and CSE in tumor biopsies from a cohort of 80 women, diagnosed with BC (Table 1). Tumors from BC patients showed significantly higher expression levels of CBS ($P = 0.0005$) and CSE ($P = 0.0019$) transcripts relative to histologically normal breast tissues isolated from the same mastectomy sample (Fig. 1a). All BC subtypes (Luminal A, luminal B, HER2 enriched and TNBC) showed elevated levels of CBS and CSE with no significant differences in the expression levels of those enzymes between the different subtypes. Moreover, serum H_2S levels were significantly higher in BC patients (28.74 ± 1.33 μM) when compared to healthy gender and age matched controls (19.94 ± 0.85 μM; $p < 0.0001$) (Fig. 1b). The elevation of serum H_2S and its synthesizing enzymes in BC patients, independent of the BC subtype, prompted us to investigate the correlation between the expression pattern of CBS and CSE with the proliferation index of BC tissues, an established prognostic marker of the disease [39]. *Interestingly,* tumors

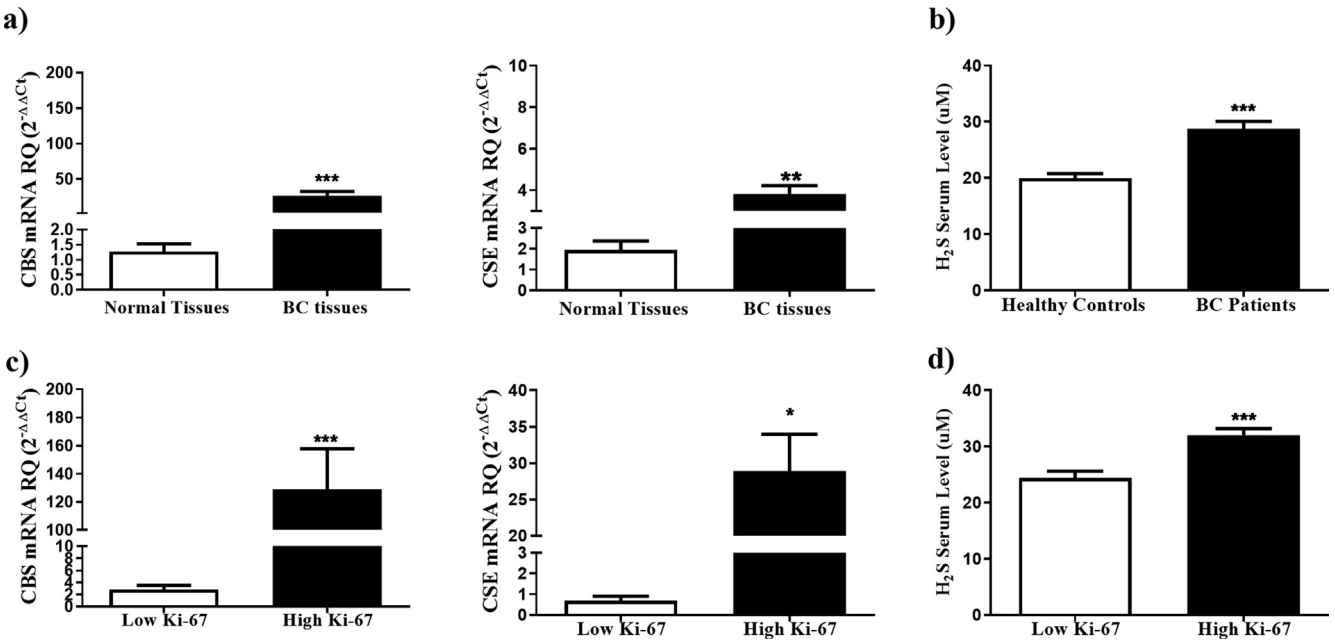

Fig. 1. Overexpression of CBS and CSE enzymes in BC tissues. (a) CBS and CSE expression profiles were analyzed in breast tissues isolated from 80 BC patients using qRT- PCR, normalized to 18 s rRNA as an internal control, and compared to normal BC tissues from the same patients (b) Serum H_2S was compared between BC patients and healthy volunteers. (c) CBS and CSE expression was compared according to the tumor proliferation index ki-67. (d) Serum H_2S levels were compared according to the tumor proliferative index ki-67.

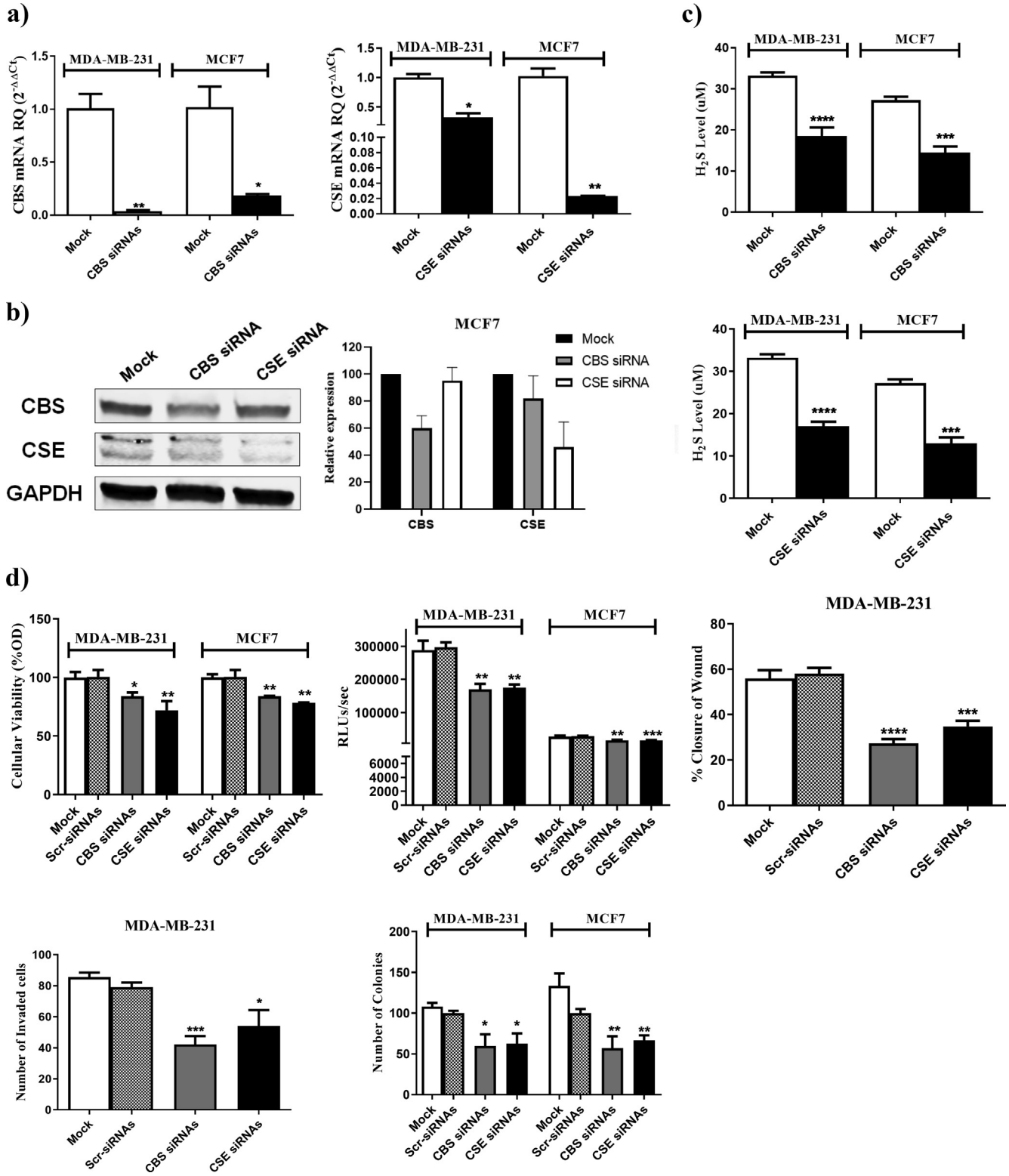

Fig. 2. CBS and CSE sequence specific siRNAs downregulate RNA, protein and H_2S production levels and impact BC malignant properties. The expression of CBS and CSE transcripts and protein levels in mock and siRNAs transfected MDA-MB-231 and MCF7 cells were determined using (a) qRT-PCR 48 h post-transfection and (b) western blot analysis 72 h post-transfection (c) H_2S levels were determined in the supernatant of MDA-MB-231 and MCF7 after silencing of CBS and CSE (d) Knocking down of CBS and CSE using CBS and CSE siRNAs resulted in a marked repression of cellular viability assessed by MTT assay (top left), cellular proliferation assessed using BrdU incorporation assay (top middle), migration capacity measured by wound healing assay (top right), invasion capacity measured by Boyder chamber assay (bottom left) and colony formation ability (bottom right).

with a high proliferation marker Ki-67 expression (≥14%) showed significantly elevated levels of CBS (P = 0.0002), CSE (P = 0.0103) (Fig. 1c) and H_2S (P = 0.0008) (Fig. 1d) compared to tumors with low Ki-67 (<14%).

Inhibition of endogenous H_2S production attenuates the malignant properties of BC cells in vitro

Since CBS and CSE were found to be elevated in various subtypes of BC, MCF7, a $HR^+/HER2^+$ BC cell line, and MDA-MB-231, a TNBC cell line, were used to analyze the impact of CBS and CSE silencing on the malignant phenotype of BC cells. Knocking down (KD) of CBS or CSE using siRNAs resulted in efficient reduction of CBS and CSE transcript and protein levels as evaluated via qRT-PCR (Fig. 2a) and western blot analysis (Fig. 2b, Supplementary Fig. S1), respectively. This was associated with a significant decrease in the H_2S levels produced by both BC cell lines (Fig. 2c). KD of CBS or CSE led to a marked reduction in BC cellular viability, proliferation, migration, invasion, and colony forming ability (Fig. 2d).

Inhibition of endogenous H_2S production modulates PI3K/Akt, JAK/STAT3 and miR-155/NOS2/NO signaling pathways in BC cells

HER2 signaling is a key mediator of the malignant phenotype of HER2 expressing BC cell lines. In order to study the underlying mechanisms for the altered tumorigenicity/malignant potential of the $HR^+/HER2^+$ MCF7 cell line, we evaluated the effect of CBS/CSE

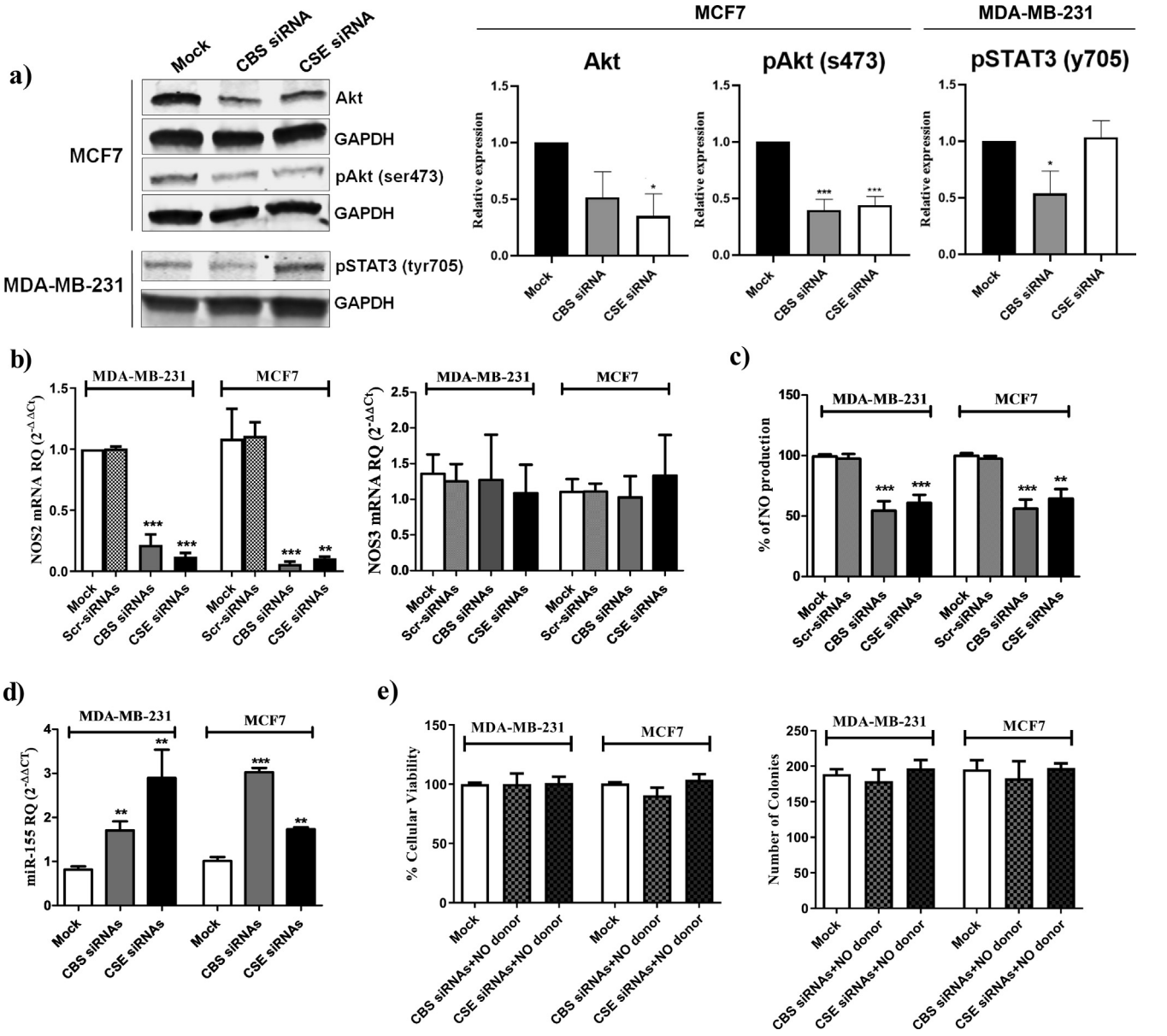

Fig. 3. CBS/CSE silencing modulates PI3K/Akt, JAK/STAT3 and miR-155/NOS2/NO signaling pathways. (a) The protein expression of Akt, phosho-Akt (serine 473) in mock or siRNA transfected MCF7 and phosphor-STAT3 (tyrosine 705) in mock or siRNA transfected MDA-MB-231 was determined using western blot 72 h post transfection. Relative expression plots were normalized to the internal control GAPDH, then compared to the mock ± standard deviation from 3 separate experiments (b) the RNA trnascripts of NOS2 and NOS3 in mock and siRNAs transfected MDA-MB-231 and MCF7 cells determined by qRT-PCR 48 h post-transfection. (c) NO levels were determined in the supernatant of MDA-MB-231 and MCF7 after silencing of CBS and CSE. (d) The expression pattern of miR-155 normalized to RNU6B as an internal control in mock, CBS siRNAs and CSE siRNAs MDA-MB-231 and MCF7 cells were determined by qRT-PCR 48 h post-transfection. (e) Cellular viability and colony forming ability of MDA-MB-231 and MCF-7 cells co-treated with a NO donor ($NaNO_2$) and CBS or CSE siRNA.

KD/silencing on the PI3K/Akt pathway which is a key HER2 signaling pathway. We found that total Akt and active phosphorylated Akt levels significantly decreased upon repression of endogenous H_2S production (Akt: CBS siRNA p = 0.092952, CSE siRNA p = 0.042246; pAkt: CBS siRNA p = 0.000366, CSE siRNA p = 0. 0.000779) (Fig. 3a, Supplementary Fig. S1). Of note, no effect on Akt and phosphorylated Akt levels was observed in the TNBC MDA-MB-231 cell line (data not shown). In TNBC, the JAK/STAT3 pathway has been reported to be an important mediator of tumorgenicity [40]. Accordingly, the effect of CBS/CSE KD on STAT3 was investigated in the TNBC cell line, MDA-MB-231, which resulted in a significant decrease in the activated/phosphorylated STAT3 levels in CBS silenced cells (Fig. 3a, Supplementary Fig. S1).

NO signaling has been associated with several malignancies including BC. We previously reported on the cross-talk between exogenous H_2S and NO pathway in TNBC [14]. We, therefore, investigated the effect of CBS/CSE silencing on NO production. *Interestingly,* CBS and CSE KD resulted in a marked repression of NOS2 transcript levels but had no significant effect on the NOS3 transcript levels (Fig. 3b). Additionally, this significantly attenuated NO production levels (Fig. 3c). The microRNA molecules: miR-146a and miR-155 were previously found to regulate the NOS2 transcript levels [41,42]. Accordingly, the expression levels of miR-146a and miR-155 were evaluated in CBS or CSE siRNA transfected BC cells. The expression of miR-155 was significantly upregulated in CBS or CSE KD BC cells (Fig. 3d), whereas miR-146a expression did not change significantly (Supplementary Fig. S2). Furthermore, co-treatment of CBS or CSE siRNA-transfected MDA-MB-231 and MCF7 cells with a NO donor ($NaNO_2$) abrogated the anti-neoplastic effects of CBS and CSE siRNAs (Fig. 3e). *Collectively*, these results propose an interaction between the endogenous H_2S and NO pathways in BC cells whereby the pro-carcinogenic effects of H_2S may be, at least in part, mediated through its effects on NO production via the miR-155/NOS2/NO signaling pathway.

Inhibition of endogenous H_2S production enhances the susceptibility of BC cells to immune-mediated killing

Tumor cells utilize various mechanisms to evade immune responses mediated by effector cells including T cells and NK cells [43,44]. The results showed that interruption of H_2S signaling via CBS/CSE silencing lead to an improvement in NK cell-mediated cytotoxicity against MDA-MB-231 (Fig. 4a) and HER2-targeting Chimeric Antigen Receptor (CAR) T cell-mediated cytotoxicity against $HR^+/HER2^+$ MCF7 cells (Fig. 4b). To explore the possible underlying mechanisms that may have contributed to the increased susceptibility to immune-mediated killing, we evaluated the effect of CBS/CSE silencing on NKG2D ligands including ULBP2 and MICA in the MDA-MB-231 cells. We observed that ULBP2 and MICA mRNA transcripts were significantly increased upon repressing the endogenous production of H_2S (Fig. 4c). Moreover, there was also a significant reduction in the level of TNF-α and an elevation in the level of interferon-γ production by MDA-MB-231 cells, which may promote a more inflammatory tumor microenvironment (Fig. 4d). In MCF7 cells, H_2S silencing led to increased expression of the T cell co-stimulatory ligands: CD80 (B7-1) / CD86 (B7-2) and 41BB ligand that activate T cell through interacting with CD28 and CD137 (41BB), respectively (Fig. 4e). Nonetheless, repression of endogenous H_2S increased expression of MHC II (HLA-DR), a molecule that has been described to mediate antigenicity to adaptive immune responses (Fig. 4e and Supplementary Fig. S3). Importantly, no significant changes were found in the expression of HER2 or the T cell inhibitory ligand, PD-L1, upon CBS or CSE silencing (Fig. 4f and Supplementary Fig. S3). *Collectively*, inhibition of endogenous H_2S production led to increased expression of activating/co-stimulatory ligands on BC cells and increased their susceptibility to NK cell- and T cell-mediated immune responses.

Identification of miR-4317 as a potential regulator of CBS and CSE in BC

Having demonstrated a possible role of CBS and CSE in modulating BC oncogenic and immunogenic profiles, we sought to explore the effect of dual targeting the CBS and CSE in BC cells. Since miRNAs possess the potential to bind and down-regulate multiple mRNA targets, we used *in-silico* prediction models to identify miRNA candidates that can simultaneously target CBS and CSE transcripts. These models identified miR-4317 as a candidate that can potentially bind to the CBS 3′-UTR sequence at two different binding regions and the CSE 3′-UTR sequence at 1 binding region with high binding scores (Supplementary Table S3 and Supplementary Fig. S4). We first examined the expression pattern of miR-4317 in primary BC specimens. miR-4317 expression level was found to be significantly lower in BC tissues as compared to normal breast tissues (P = 0.0017) (Fig. 5a). Additionally, it was significantly lower in TNBC specimens when compared to other BC subtypes (P < 0.0001) (Fig. 5b). In a similar pattern, the TNBC cell line, MDA-MB-231, exhibited levels of miR-4317 lower than the $HR^+/HER2^+$ MCF7 cell line (P < 0.0001) (Fig. 5c), a phenotype that could be reversed in both MCF7 and MDA-MB-231 by ectopic expression of miR-4317 using miR-4317 mimics (Fig. 5d).

miR-4317 directly co-targets CBS and CSE in BC and inhibits its malignant phenotype

To assess whether miR-4317 directly targets the 3′-UTR of CBS and CSE, a dual luciferase assay was used. Luciferase-expressing constructs were prepared and incorporated in it the predicted miR-4317-CBS binding sites 1or 2, or the miR-4317-CSE binding site as indicated in Supplementary Table S2. These constructs were either transfected alone or with the miR-4317-expressing construct. In the presence of miR-4317, the luciferase-expressing constructs containing the miR-4317-CBS binding site 2 and the miR-4317-CSE binding site showed markedly lower levels of luciferase activity compared to cells transfected with the luciferase-expressing constructs alone. No significant reduction in the luciferase activity was detected for the construct containing the miR-4317-CBS binding site 1 when co-transfected with miR-4317 (Fig. 6a). Ectopic expression of miR-4317 in the two BC cell lines resulted in a marked repression of CBS and CSE transcript levels (Fig. 6b), alongside a reduction in H_2S production levels (Fig. 6c). This also led to a significant reduction in BC cellular viability, proliferation and colony formation in both BC cell lines in a manner comparable to CBS/CSE siRNAs co-transfection (Fig. 6d). Moreover, a decrease in the cellular migration and invasion of the aggressive TNBC cell line, MDA-MB-231, was noted following miR-4317 induced expression (Fig. 6e).

Discussion

Gasotransmitters, including H_2S, are emerging as potential mediators in different pathological conditions and as possible diagnostic and prognostic markers in cancer [45,46]. The synthesizing enzymes of those gasotransmitters were recently discovered to be significantly altered in tumor tissues, suggesting a potential role in the process of carcinogenesis [45]. Published studies in colon and ovarian cancer demonstrated the up-regulation of CBS in primary tumors and that CBS seems to be the predominant source of endogenous H_2S. In the present study we observed that both CBS and CSE were up-regulated in clinical samples from primary

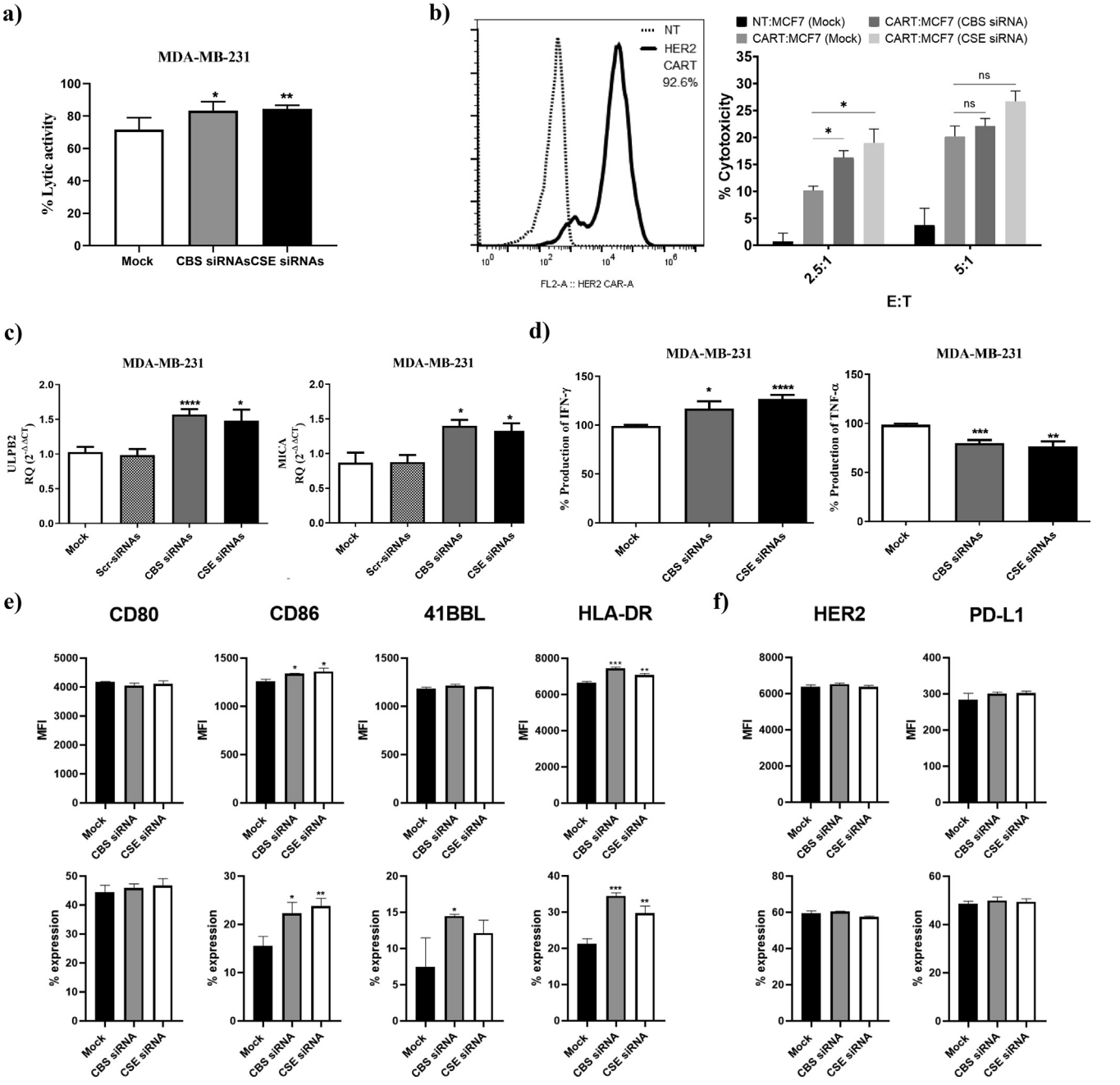

Fig. 4. Impact of silencing CBS and CSE on immune cell mediated cytotoxicity, immune ligand expression and cytokines release. (a) NK cell mediated cytotoxicity was tested via co-culturing experiments that were done between mock, CBS/CSE KDMDA-MB-231 and primary NK cells using LDH assay. (b) T cell mediated cytotoxicity was tested using HER2 targeting CAR T cells. CAR transduction rate was tested using a recombinant human ErbB2/Her2 Fc chimeric protein + PE-conjugated goat anti-human IgG (Fc gamma-specific) andcompared to non-transduced (NT) T cells. CAR T cell mediated cytotoxicity was tested by a chromium (^{51}Cr) release assay. CAR T cells were incubated with MCF7 cells at effector to target ratios of 2.5:1 and 5:1 for 6 h. Cytotoxicity is presented as percentage normalized to triton-X induced cytotoxicity.(c) ULBP2 and MICA were analyzed on the mRNA transcripts level in mock, CBS or CSE KD MDA-MB-231 using qRT-PCR 48 h post-transfection. (d) The supernatant of mock, CBS/CSE KD MDA-MB-231 was screened for IFN-γ and TNF-α production using ELISA. (e) CD80, CD86, 41BBL and HLA-DR surface expression on mock, CBS or CSE KD MCF7, represented as percentage expression and median fluorescence intensity, were analyzed using flow cytometry 72 h post-transfection (f) HER2 and PD-L1 surface expression on mock, CBS/CSE KD MCF7, represented as percentage expression and median fluorescence intensity, was analyzed using flow cytometry 72 h post-transfection.

BC patients and that both contribute to H_2S production in BC cells. Similarly, others have shown elevated levels of CBS and CSE in hepatoma cell lines [47] and bladder urothelial cell carcinoma [48]. In this study, we demonstrate a marked attenuation of key measures of aggressiveness of BC cell lines upon CBS and/or CSE knock-down supporting a possible role of H_2S synthesis in mediating the malignant phenotype of BC cells. Other studies have also shown that silencing CBS and CSE can alter the progression of several malignancies [18,19,48].

Silencing of the H_2S synthetic pathway impacted the tumorgenicity of MDA-MB-231 (TNBC) and MCF-7 ($HR^+/HER2^+$) cell lines via distinct mechanisms. In MCF7 cells, CBS/CSE silencing resulted in a marked down-regulation of Akt and phosphorylated Akt. The importance of the PI3K/Akt pathway in the MCF7 cell line is further supported by a previous report showing that inhibition of this pathway in MCF7 had a negative impact on cell survival, but did not significantly affect the survival of the TNBC cell line, MDA-MB-231 [49]. On the other hand, MDA-MB-231 cells onco-

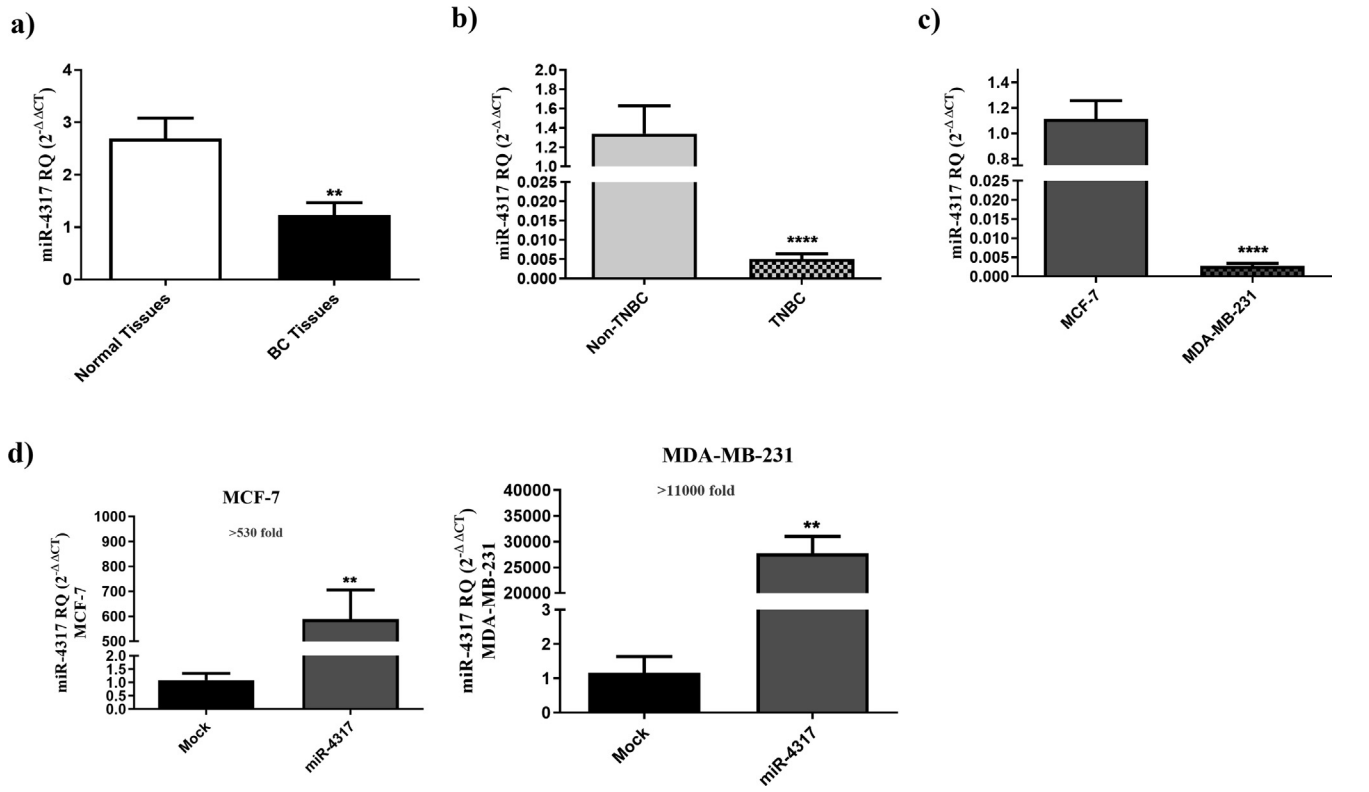

Fig. 5. miR-4317 is downregulated in TNBC clinical samples and cell line. (a) miR-4317 expression profile was analyzed in tumor tissues from 80 BC patients and compared to patient matched normal tissues using qRT-PCR, and normalized to RNU6B as an internal control. (b) Repressed expression levels of miR-4317 in TNBC patients compared to non-TNBC patients, (c) Reduced expression levels of miR-4317 in MDA-MB-231 cell line when compared to MCF7 cells. The expression of miR-4317 in MDA-MB-231 and MCF7 cells was determined by qRT-PCR 48 h post-transfection. (d) Levels of miR-4317 showed more than 530 folds increase in miR-4317 plasmid transfected MCF7 cells compared to mock cells. miR-4317 plasmid transfected MDA-MB-231 cells showed more than 11,000 folds increase in the expression level of miR-4317 when compared to mock cells, determined by qRT-PCR 48 h post-transfection.

genicity was reported to be more dependent on the cytokine receptor-mediated JAK/STAT signaling [40]. Therefore, decreased phosphorylated STAT3 levels in MDA-MB-231 cells following CBS/CSE silencing in this study may partly explain the observed attenuation of MDA-MB-231 malignant phenotype.

Recently, our group has reported a tangled crosstalk between "exogenous" H_2S and endogenous NO production in TNBC cells through the sONE/NOS3 axis [14]. Of note, in this study we investigated the possible relationship between the CBS/CSE induced H_2S production in BC cells and the NO pathway. It was evident that the biological effects of endogenous H_2S in both BC cell lines are, in part, mediated by NO. However, compared to exogenous H_2S, the intrinsic mechanism underlying this crosstalk seems to be different. While exogenous H_2S mediates its effect through the sONE/NOS3/NO axis [14], the results of this study showed that endogenous H_2S mediates its effects mainly through the miR-155/NOS2/NO axis. This is concordant with the recently reported role of several miRNAs in transducing endogenous H_2S signaling [50,51]. *Altogether*, this study demonstrated that CBS/CSE induced H_2S production has been implicated with PI3k/Akt/mTOR, JAK/STAT and miR-155/NOS2/NO signaling pathways.

Tumor immunogenicity and the role of NK cells and cytotoxic T lymphocytes in mediating anti-tumor immune responses have been extensively investigated [52–54]. Targeting NKG2D ligands and/or blocking PD-1/PD-L1 interactions (checkpoint inhibitors) have been the subject of clinical research and application [55,56]. Since alterations in the miR-155/NOS2/NO signaling pathway have been reported to attenuate the immune suppressive tumor microenvironment [31,57–59], we hypothesized that endogenous H_2S may modulate the immunogenic profile of BC cells. Tumor cells tend to down-regulate NKG2D ligands through intracellular retention and/or extracellular shedding to evade NKG2D receptor-mediated NK cell killing. Interestingly, CBS and CSE silencing induced the expression of the NKG2D ligands, MICA and ULBP2, in the MDA-MD-231 TNBC cell line. This was associated with improved NK cell cytotoxicity against H_2S-depleted tumor targets. These findings are concordant with the CBS/CSE KD associated attenuation of STAT3, which was described as a transcriptional repressor of the NKG2D ligands, MICA/B and ULBP2, in colon cancer, liver cancer and multiple myeloma [28,60]. Furthermore, CBS and CSE siRNAs led to a reduced production of TNF-α, a cytokine that may contribute to immune cell apoptosis within the tumor microenvironment. Interestingly, a recent report highlighted the role of H_2S in tuning the levels of several pro-inflammatory cytokines including TNF-α in diabetic rat model [61].

On the other hand, silencing of CBS and CSE led to improved killing of the $HR^+/HER2^+$ MCF7 cells by anti-HER2 CAR T cells. This may have been partly mediated by the up-regulation of co-stimulatory ligands, including CD86 (B7-2) and 4-1BB ligand (41BBL), on MCF7 cells since the binding of these ligands to their cognate receptors (CD28 and 4-1BB) on T cells is critical for effective T cell activation and function [62,63]. Of note, the increase in the expression of HLA-DR (class II MHC), which may expose mutant epitopes render tumor cell more immunogenic [43,64], and co-stimulatory ligands [65] on MCF7 cells as well as the changes in NK ligands and cytokine secretion by MDA-MD-231 cells following CBS/CSE KD may be conducive of more effective immune responses against BC cells.

Finally, in an attempt to simultaneously target CBS and CSE using a novel miRNA to halt BC progression, we found that miR-4317 can

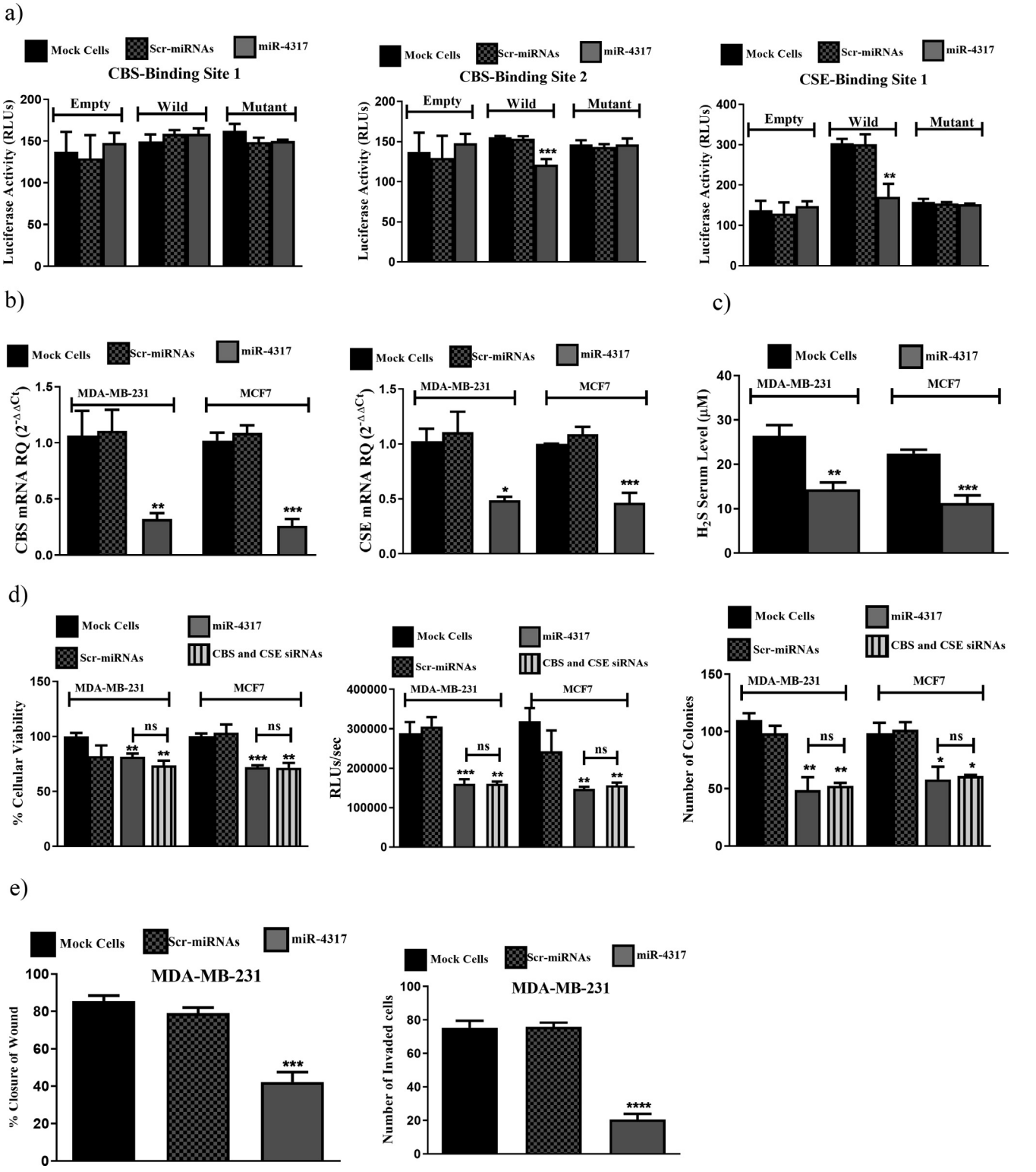

Fig. 6. miR-4317 co-targets CBS and CSE simultaneously mitigating BC malignant properties. (a) Luciferase reporter assay for binding confirmation of miR-4317 on 3′UTR of CBS and CSE. miR-4317-CBS first binding site construct showed no inhibition of luciferase activity. miR-4317-CBS second binding site construct showed significant reduction of luciferase activity in cells co-transfected with miR-4317 mimics plus WT construct compared to mock and scr-miRNAs transfected cells transfected with the WT construct alone. Likewise, for the miR-4317-CSE binding site construct, luciferase activity was also significantly repressed in cells co-transfected with miR-4317 mimics plus WT construct compared to mock and scr-miRNAs transfected cells transfected with the WT construct alone. (b) Down-regulation of CBS and CSE expression by miR-4317 mimics in MDA-MB-231 and MCF7 cells. (c) Reduced H_2S levels produced from BC cells upon transfection with miR-4317 mimics. (d) miR-4317 mimics reduced cellular viability (left), cellular proliferation (middle), and colony formation ability (right) in MDA-MB-231 and MCF7. (e) miR-4317 mimics resulted in reduction in migration (left) and invasion (right) capacities in MDA-MB-231.

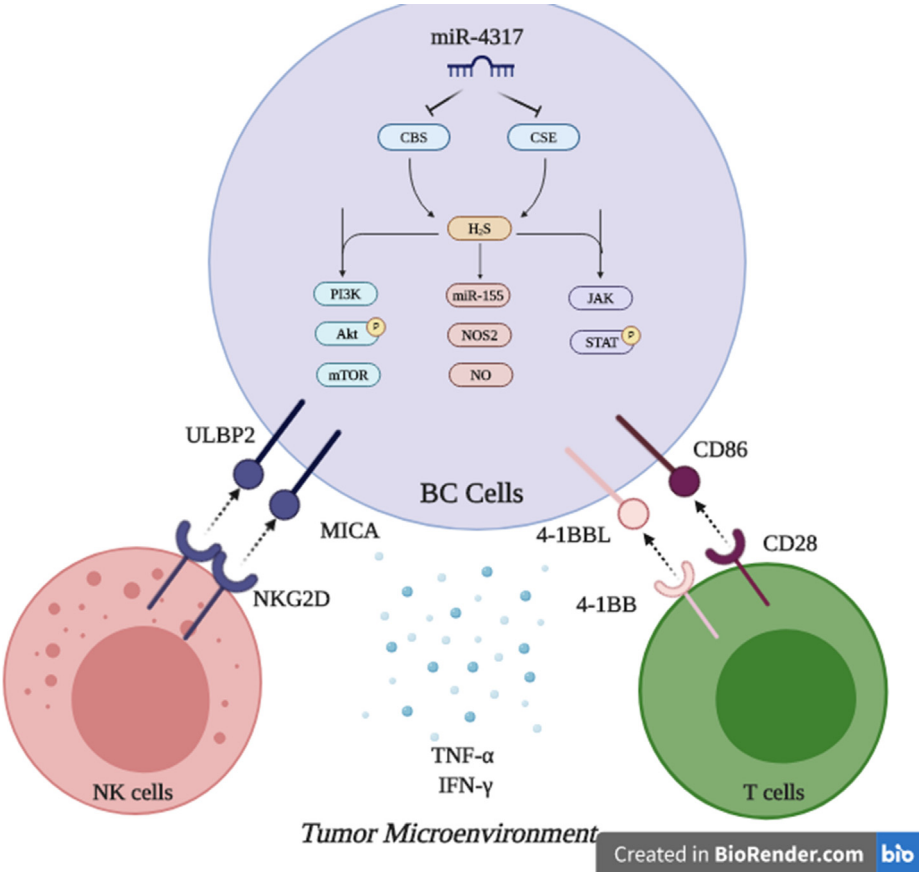

Fig. 7. . Targeting H_2S synthesizing machinery in BC cells. This is a conclusive descriptive figure highlighting the major roles of endogenously produced H_2S in BC cells. Mechanistically, PI3K/Akt/mTOR, miR-155/NOS2/NO, JAK/STAT can be drawn downstream CBS and CSE induced H_2S in BC cells. Functionally, this results in abrogation of BC hallmarks, potentiating NK cells and cytotoxic T cells activity and alleviating the immune suppressive microenvironment in BC tumors. Dual Targeting of CBS and CSE in BC cells was achieved using the novel tumor suppressor miR-4317.

potentially target both CBS and CSE transcripts through *in silico* analysis and this was functionally confirmed using a luciferase-based assay. This adds miR-4317 to the list of validated miRNAs that modulate the endogenous production of H_2S along with miR-21 [66], miR-22 [67] and miR-30 [68]. Yet, all the previously reported H_2S-modulating miRNAs directly target CSE. However, to our knowledge, CBS has not been described as a direct target for miRNAs. Thus, miR-4317 is the first validated miRNA to co-target CBS and CSE simultaneously. While miR-4317 tumor suppressor activity has only been reported in gastric carcinoma [69], this is the first study to describe the tumor suppressor activity of miR-4317 in BC. Noteworthy, results confirmed that miR-4317 was significantly down-regulated in TNBC patients compared to other BC subtypes. Therefore, the consideration of miR-4317 as a possible diagnostic or prognostic marker in TNBC warrants further validation. Additionally, targeted therapies aimed at up-regulating tumor suppressor miRNAs [70] such as miR-4317 expression may have important anti-tumor activities and may be particularly appealing considering the lack of targeted therapies and the dissatisfactory outcomes in TNBC. *In conclusion,* this study revealed that tissue levels of CBS and CSE were associated with high proliferation index in clinical samples, suggesting a prognostic value of these enzymes. Inhibition of the H_2S synthesizing enzymes suppresses BC oncogenicity, as evident by its effect on cell proliferation, survival, invasion, and migration, and increases their susceptibility to both innate and adaptive cellular immune responses. Finally, miR-4317 was portrayed as a novel tumor suppressor miRNA in BC that acts through simultaneous repression of CBS and CSE (Fig. 7).

Compliance with ethics requirements

All procedures followed were in accordance with the ethical standards of the responsible committee on human experimentation (institutional and national) and with the Helsinki Declaration of 1975, as revised in 2008 (5). Informed consent was obtained from all patients for being included in the study.

Ethics declarations

Ethics approval and consent to participate

Ethical approvals were obtained from the ethical committees of German University in Cairo, Cairo University and written informed consent was obtained from each patient and normal individual.

Availability of supporting data

All supporting data are available with their detailed descriptions.

Consent for publication

The authors asked for full waiver for publication fees due to funds limitations.

Authors' contributions

The research conception and design was done by RAY and MZG. RAY, AZG, and KS completed data acquisition, and analysis. Interpretation of data was performed by RAY, AZG, KS, NA, AAM, and MZG. Clinical data of BC patients was provided by EK an HMH. The H_2S detection plates were designed/supplied by YJA and GJL. Writing, review, and/or revision of the manuscript were done by RAY, AZG, KS, NA, AAM, and MZG. NA, AAM, and MZG provided study supervision.

Declaration of Competing Interest

The authors declare that they have no known competing financial interests or personal relationships that could have appeared to influence the work reported in this paper.

Acknowledgements

This work was supported by the Stand Up to Cancer–St Baldrick's Pediatric Dream Team Translational Research Grant (SU2C-AACR-DT1113). Stand Up to Cancer is a program of the Entertainment Industry Foundation administered by the American Association for Cancer Research.

Appendix A. Supplementary material

Supplementary data to this article can be found online at https://doi.org/10.1016/j.jare.2020.07.006.

References

[1] Waks AG, Winer EP. Breast cancer treatment: a review. JAMA 2019;321(3):288–300.
[2] Bray F et al. Global cancer statistics 2018: GLOBOCAN estimates of incidence and mortality worldwide for 36 cancers in 185 countries. CA Cancer J Clin 2018;68(6):394–424.
[3] Nielsen DL et al. Efficacy of HER2-targeted therapy in metastatic breast cancer. Monoclonal antibodies and tyrosine kinase inhibitors. Breast 2013;22(1):1–12.
[4] Denkert C et al. Molecular alterations in triple-negative breast cancer-the road to new treatment strategies. Lancet 2017;389(10087):2430–42.
[5] Youness RA, Gad MZ. Long non-coding RNAs: Functional regulatory players in breast cancer. Noncoding RNA Res 2019;4(1):36–44.
[6] Youness RA et al. The long noncoding RNA sONE represses triple-negative breast cancer aggressiveness through inducing the expression of miR-34a, miR-15a, miR-16, and let-7a. J Cell Physiol 2019;234(11):20286–97.
[7] Ibrahim AS et al. Cancer incidence in egypt: results of the national population-based cancer registry program. J Cancer Epidemiol 2014;2014:437971.
[8] Ferlay J et al. Cancer incidence and mortality worldwide: sources, methods and major patterns in GLOBOCAN 2012. Int J Cancer 2015;136(5):E359–86.
[9] Ataollahi F et al. Evaluation of copper concentration in subclinical cases of white muscle disease and its relationship with cardiac troponin I. PLoS ONE 2013;8(2):e56163.
[10] Wu DD et al. Hydrogen sulfide as a novel regulatory factor in liver health and disease. Oxid Med Cell Longev 2019;2019:3831713.
[11] Dong Q et al. A novel hydrogen sulfide-releasing donor, HA-ADT, suppresses the growth of human breast cancer cells through inhibiting the PI3K/AKT/mTOR and Ras/Raf/MEK/ERK signaling pathways. Cancer Lett 2019;455:60–72.
[12] Wang L et al. I157172, a novel inhibitor of cystathionine gamma-lyase, inhibits growth and migration of breast cancer cells via SIRT1-mediated deacetylation of STAT3. Oncol Rep 2019;41(1):427–36.
[13] You J et al. Cystathionine- gamma-lyase promotes process of breast cancer in association with STAT3 signaling pathway. Oncotarget 2017;8(39):65677–86.
[14] Youness RA et al. A novel role of sONE/NOS3/NO signaling cascade in mediating hydrogen sulphide bilateral effects on triple negative breast cancer progression. Nitric Oxide 2018;80:12–23.
[15] Youness RA et al. The long noncoding RNA sONE represses triple-negative breast cancer aggressiveness through inducing the expression of miR-34a, miR-15a, miR-16, and let-7a. J Cell Physiol 2019.
[16] Brahmer JR et al. Safety and activity of anti-PD-L1 antibody in patients with advanced cancer. N Engl J Med 2012;366(26):2455–65.
[17] Zhu H et al. Cystathionine beta-synthase in physiology and cancer. Biomed Res Int 2018;2018:3205125.
[18] Bhattacharyya S et al. Cystathionine beta-synthase (CBS) contributes to advanced ovarian cancer progression and drug resistance. PLoS ONE 2013;8(11):e79167.
[19] Szabo C et al. Tumor-derived hydrogen sulfide, produced by cystathionine-beta-synthase, stimulates bioenergetics, cell proliferation, and angiogenesis in colon cancer. Proc Natl Acad Sci U S A 2013;110(30):12474–9.
[20] Kim J et al. Expression of cystathionine beta-synthase is downregulated in hepatocellular carcinoma and associated with poor prognosis. Oncol Rep 2009;21(6):1449–54.
[21] Fan K et al. Wnt/beta-catenin signaling induces the transcription of cystathionine-gamma-lyase, a stimulator of tumor in colon cancer. Cell Signal 2014;26(12):2801–8.
[22] Cai WJ et al. Hydrogen sulfide induces human colon cancer cell proliferation: role of Akt, ERK and p21. Cell Biol Int 2010;34(6):565–72.
[23] Cao Q et al. Butyrate-stimulated H2S production in colon cancer cells. Antioxid Redox Signal 2010;12(9):1101–9.
[24] Pan Y et al. Hydrogen sulfide (H2S)/cystathionine gamma-lyase (CSE) pathway contributes to the proliferation of hepatoma cells. Mutat Res 2014;763–764:10–8.
[25] Yin P et al. Sp1 is involved in regulation of cystathionine gamma-lyase gene expression and biological function by PI3K/Akt pathway in human hepatocellular carcinoma cell lines. Cell Signal 2012;24(6):1229–40.
[26] Pei Y et al. Hydrogen sulfide mediates the anti-survival effect of sulforaphane on human prostate cancer cells. Toxicol Appl Pharmacol 2011;257(3):420–8.
[27] Youness RA et al. A methoxylated quercetin glycoside harnesses HCC tumor progression in a TP53/miR-15/miR-16 dependent manner. Nat Prod Res 2018:1–6.
[28] Youness RA et al. Contradicting interplay between insulin-like growth factor-1 and miR-486-5p in primary NK cells and hepatoma cell lines with a contemporary inhibitory impact on HCC tumor progression. Growth Factors 2016;34(3–4):128–40.
[29] Awad AR et al. An acetylated derivative of vitexin halts MDA-MB-231 cellular progression and improves its immunogenic profile through tuning miR- 20a-MICA/B axis. Nat Prod Res 2019:1–5.
[30] Youness RA et al. MicroRNA-486-5p enhances hepatocellular carcinoma tumor suppression through repression of IGF-1R and its downstream mTOR, STAT3 and c-Myc. Oncol Lett 2016;12(4):2567–73.
[31] Aboelenein HR et al. Reduction of CD19 autoimmunity marker on B cells of paediatric SLE patients through repressing PU.1/TNF-alpha/BAFF axis pathway by miR-155. Growth Factors 2017;35(2–3):49–60.
[32] Ahmed Youness R et al. A methoxylated quercetin glycoside harnesses HCC tumor progression in a TP53/miR-15/miR-16 dependent manner. Nat Prod Res 2020;34(10):1475–80.
[33] Youssef SS et al. PNPLA3 and IL 28B signature for predicting susceptibility to chronic hepatitis C infection and fibrosis progression. Arch Physiol Biochem 2019:1–7.
[34] Mekky RY et al. Epigallocatechin gallate (EGCG) and miR-548m reduce HCV entry through repression of CD81 receptor in HCV cell models. Arch Virol 2019;164(6):1587–95.
[35] Kim TJ et al. Characterization of H2S releasing properties of various H2S donors utilizing microplate cover-based colorimetric assay. Anal Biochem 2019;574:57–65.
[36] Ahn YJ et al. Colorimetric detection of endogenous hydrogen sulfide production in living cells. Spectrochim Acta A Mol Biomol Spectrosc 2017;177:118–24.
[37] Rahmoon MA et al. MiR-615-5p depresses natural killer cells cytotoxicity through repressing IGF-1R in hepatocellular carcinoma patients. Growth Factors 2017;35(2–3):76–87.
[38] Shaalan YM et al. Destabilizing the interplay between miR-1275 and IGF2BPs by Tamarix articulata and quercetin in hepatocellular carcinoma. Nat Prod Res 2018;32(18):2217–20.
[39] Chen X et al. The predictive value of Ki-67 before neoadjuvant chemotherapy for breast cancer: a systematic review and meta-analysis. Future Oncol 2017;13(9):843–57.
[40] Yang Y et al. Ganoderic acid A exerts antitumor activity against MDA-MB-231 human breast cancer cells by inhibiting the Janus kinase 2/signal transducer and activator of transcription 3 signaling pathway. Oncol Lett 2018;16(5):6515–21.
[41] Xin H et al. Hydrogen sulfide attenuates inflammatory hepcidin by reducing IL-6 secretion and promoting SIRT1-mediated STAT3 deacetylation. Antioxid Redox Signal 2016;24(2):70–83.
[42] Yao Y et al. Inflammatory response of macrophages cultured with Helicobacter pylori strains was regulated by miR-155. Int J Clin Exp Pathol 2015;8(5):4545–54.
[43] Axelrod ML et al. Biological consequences of MHC-II expression by tumor cells in cancer. Clin Cancer Res 2019;25(8):2392–402.
[44] Driessens G, Kline J, Gajewski TF. Costimulatory and coinhibitory receptors in anti-tumor immunity. Immunol Rev 2009;229(1):126–44.
[45] Szabo C. Gasotransmitters in cancer: from pathophysiology to experimental therapy. Nat Rev Drug Discov 2016;15(3):185–203.
[46] Wu D et al. Hydrogen sulfide in cancer: Friend or foe?. Nitric Oxide 2015;50:38–45.
[47] Zhen Y et al. Exogenous hydrogen sulfide exerts proliferation/anti-apoptosis/angiogenesis/migration effects via amplifying the activation of NF-kappaB pathway in PLC/PRF/5 hepatoma cells. Int J Oncol 2015;46(5):2194–204.
[48] Gai JW, et al. Expression profile of hydrogen sulfide and its synthases correlates with tumor stage and grade in urothelial cell carcinoma of bladder. Urol Oncol, 2016. 34(4): p. 166 e15-20.
[49] Marina M, Wang L, Conrad SE. The scaffold protein MEK Partner 1 is required for the survival of estrogen receptor positive breast cancer cells. Cell Commun Signal 2012;10(1):18.
[50] Hu TX et al. MiR 20a,-20b and -200c are involved in hydrogen sulfide stimulation of VEGF production in human placental trophoblasts. Placenta 2016;39:101–10.
[51] Zhou Y et al. Hydrogen sulfide promotes angiogenesis by downregulating miR-640 via the VEGFR2/mTOR pathway. Am J Physiol Cell Physiol 2016;310(4):C305–17.
[52] Sun H, Sun C. The rise of NK cell checkpoints as promising therapeutic targets in cancer immunotherapy. Front Immunol 2019;10:2354.
[53] Ihara F et al. Regulatory T cells induce CD4(-) NKT cell anergy and suppress NKT cell cytotoxic function. Cancer Immunol Immunother 2019.

[54] Jiang J, Natarajan K, Margulies DH. MHC molecules, T cell receptors, natural killer cell receptors, and viral immunoevasins-key elements of adaptive and innate immunity. Adv Exp Med Biol 2019;1172:21–62.
[55] Garrido F et al. The urgent need to recover MHC class I in cancers for effective immunotherapy. Curr Opin Immunol 2016;39:44–51.
[56] Spear P et al. NKG2D ligands as therapeutic targets. Cancer Immun 2013;13:8.
[57] Fahim Golestaneh A et al. Large scale in vivo micro-RNA loss of function screen identified miR-29a, miR-100 and miR-155 as modulators of radioresistance and tumor-stroma communication. Int J Cancer 2019;144(11):2774–81.
[58] Huffaker TB et al. Antitumor immunity is defective in T cell-specific microRNA-155-deficient mice and is rescued by immune checkpoint blockade. J Biol Chem 2017;292(45):18530–41.
[59] Poles WA et al. Targeting the polarization of tumor-associated macrophages and modulating mir-155 expression might be a new approach to treat diffuse large B-cell lymphoma of the elderly. Cancer Immunol Immunother 2019;68 (2):269–82.
[60] Zingoni A et al. NKG2D and Its Ligands: "One for All, All for One". Front Immunol 2018;9:476.
[61] Liu M et al. Hydrogen sulfide attenuates myocardial fibrosis in diabetic rats through the JAK/STAT signaling pathway. Int J Mol Med 2018;41 (4):1867–76.
[62] Kawalekar OU et al. Distinct signaling of coreceptors regulates specific metabolism pathways and impacts memory development in CAR T cells. Immunity 2016;44(2):380–90.
[63] Velasquez MP et al. CD28 and 41BB costimulation enhances the effector function of CD19-specific engager T cells. Cancer Immunol Res 2017;5 (10):860–70.
[64] Kreiter S et al. Mutant MHC class II epitopes drive therapeutic immune responses to cancer. Nature 2015;520(7549):692–6.
[65] Sharma RK et al. Tumor cells engineered to codisplay on their surface 4–1BBL and LIGHT costimulatory proteins as a novel vaccine approach for cancer immunotherapy. Cancer Gene Ther 2010;17(10):730–41.
[66] Cindrova-Davies T et al. Reduced cystathionine gamma-lyase and increased miR-21 expression are associated with increased vascular resistance in growth-restricted pregnancies: hydrogen sulfide as a placental vasodilator. Am J Pathol 2013;182(4):1448–58.
[67] Wang L et al. MiR-22/Sp-1 links estrogens with the up-regulation of cystathionine gamma-lyase in myocardium, which contributes to estrogenic cardioprotection against oxidative stress. Endocrinology 2015;156 (6):2124–37.
[68] Shen Y et al. miRNA-30 family inhibition protects against cardiac ischemic injury by regulating cystathionine-gamma-lyase expression. Antioxid Redox Signal 2015;22(3):224–40.
[69] Hu X et al. miRNA-4317 suppresses human gastric cancer cell proliferation by targeting ZNF322. Cell Biol Int 2017.
[70] ElKhouly AM, Youness RA, Gad MZ. MicroRNA-486-5p and microRNA-486-3p: Multifaceted pleiotropic mediators in oncological and non-oncological conditions. Noncoding RNA Res 2020;5(1):11–21.